# Northumbria Research Link

Citation: Balocco, Claudio, Dodd, Linzi and Etor, David (2022) High-Performance Atomic Layer Deposited Al2O3 Insulator Based Metal-Insulator-Metal Diode. FUOYE Journal of Engineering and Technology, 7 (2). pp. 174-178. ISSN 2579-0617

Published by: UNSPECIFIED

URL: https://doi.org/10.46792/fuoyejet.v7i2.815 <https://doi.org/10.46792/fuoyejet.v7i2.815>

This version was downloaded from Northumbria Research Link: https://nrl.northumbria.ac.uk/id/eprint/51230/

Northumbria University has developed Northumbria Research Link (NRL) to enable users to access the University's research output. Copyright © and moral rights for items on NRL are retained by the individual author(s) and/or other copyright owners. Single copies of full items can be reproduced, displayed or performed, and given to third parties in any format or medium for personal research or study, educational, or not-for-profit purposes without prior permission or charge, provided the authors, title and full bibliographic details are given, as well as a hyperlink and/or URL to the original metadata page. The content must not be changed in any way. Full items must not be sold commercially in any format or medium without formal permission of the copyright holder. The full policy is available online: http://nrl.northumbria.ac.uk/policies.html

This document may differ from the final, published version of the research and has been made available online in accordance with publisher policies. To read and/or cite from the published version of the research, please visit the publisher's website (a subscription may be required.)

Northumbria University NEWCASTLE

CUSTOMER SERVICE EXCELLENCE CSE UniversityLibrary

# High-Performance Atomic Layer Deposited $Al_2O_3$ Insulator Based Metal-Insulator-Metal Diode

*[1]David Etor, [2]Linzi E. Dodd and [3]Claudio Balocco
[1]Department of Electrical and Electronics, University of Jos, Nigeria
[2]Smart Materials and Surfaces Laboratory, Northumbria University, Newcastle Upon-Tyne, United Kingdom
[3]School of Engineering and Computing Sciences, Durham University, Durham, United Kingdom
**etord@unijos.edu.ng|linzi.dodd@northumbria.ac.uk|claudio.balocco@durham.ac.uk**

Received: 03-MAR-2022; Reviewed: 25-MAR-2022; Accepted: 15-APR-2022
https://doi.org/10.46792/fuoyejet.v7i2.815

**ORIGINAL RESEARCH ARTICLE**

**Abstract-** The fabrication of metal–insulator–metal (MIM) diode using an ultrathin $Al_2O_3$ insulator layer, deposited using atomic layer deposition (ALD) is presented. The $Al_2O_3$ insulating layer was found to be highly uniform throughout the diode junction, effectively overcoming the main fabrication challenge in MIM diodes. The diodes exhibit strong non-linear current–voltage curves, have a typical zero-bias curvature coefficient of 5.4 $V^{-1}$ and a zero-bias resistance of approximately 118 kΩ, a value considerably smaller than other MIM diode topologies and that allows more current to be rectified. Other results including current ratio and yield of the diode also competes favourably with the state-of-the-art MIM diodes such as the recently produced metal-octadecyltrichlorosilane (OTS)-metal structure.

**Keywords-** Atomic Layer Deposition, Conformal insulator, Metal-insulator-metal diodes, Zero-bias curvature coefficient.

## 1 Introduction

The metal-insulator-metal (MIM) diode is a quantum device consisting of a thin insulator deposited between two thin metal electrode films with different work functions, which cause an asymmetric electric current to flow through the insulator with respect to the polarity of the electrodes and can operate at frequencies well into the infrared range (Sakuma & Evenson, 1974; Evenson et al., 1970; Drullinger et al., 1983; Denisov et al., 2007; Evenson et al., 1984). As a result, the device is useful in a broad range of applications, including wireless power transfer such as in intraocular pressure (IOP) measurement soft-contact lens and radio-frequency identification (RFID) tags, thermal-energy harvesting, and high frequency detectors (Jinpeng et al., 2012; Pan et al., 2014; Periasamy et al., 2011).

The main problem with the manufacturing of MIM diodes is the uniform insulator deposition, as a very thin insulator layer, not more than 4 nm, equivalent to a few atomic layers, must be utilized. Due to the deposition technique mostly used, such as sputtering, exposure to ambient environment, reactive ion etching (RIE) and exposure to a moist elevated temperature environment (Dodd et al., 2012), this often results in a defective layer of insulator film with many pin holes, which causes short-circuit to occur in the diode terminals and drastically reduces throughput. To overcome this problem, the development of a MIM diode in which organometallic molecules self-assembles in an insulating monolayer was reported (Etor et al., 2016).

*Corresponding Author

**Section B- ELECTRICAL/ COMPUTER ENGINEERING & RELATED SCIENCES**
**Can be cited as:**
Etor D., Dodd L.E. and Balocco C. (2022): High-Performance Atomic Layer Deposited Al2O3 Insulator Based Metal-Insulator-Metal Diode, *FUOYE Journal of Engineering and Technology* (FUOYEJET), 7(2), 174-178. http://doi.org/10.46792/fuoyejet.v7i2.815

The diode utilized an octadecyltrichlorosilane (OTS) self-assembled monolayer (SAM), which consists of carbon chains strongly packed together with an overall thickness of approximately 2 nm. Due to the nature of the self-assembly, a second layer cannot grow on top of the first one, resulting in a uniform thickness over large areas determined by the SAM chemistry (Etor et al., 2016; Etor et al., 2019). The structure of our MIM diode in (Etor et al., 2016) is titanium-octadecyltrichlorosilane-platinum (Ti/OTS/Pt) and the electrical results obtained upon characterization, such as current–voltage characteristics, zero-bias curvature coefficient, zero-bias resistance, and electron conduction, competes favourably with the state-of-the-art (Mitrovic et al., 2021; Hemmetter et al., 2021; Etor et al., 2019).

In this work, further improvements to the (electrical) performance and throughput of MIM diodes available in literature is reported. Here, atomic layer deposition (ALD), an emerging thin film deposition technique has been used to define 2 nm thick $Al_2O_3$ insulating layer in-between titanium and platinum metal films, forming a $Ti/Al_2O_3/Pt$ MIM structure with stronger nonlinear current–voltage (*J-V*) characteristic and higher throughput than that of the Ti/OTS/Pt structure previously reported in (Etor et al., 2016).

## 2 Methodology

### 2.1 Atomic Layer Deposition (ALD)

ALD is a method used in the deposition of high-quality thin films (up to a few nm) of diverse materials, including metals (Griffiths et al., 2016; Gordon et al., 2015; Niskanen et al., 2007; Chalker et al., 2010; Kariniemi et al., 2011) and metal-oxides (Wang et al., 2008; Hausmann et al., 2002; Kukli et al., 2000), with an accurate number of atomic layers, on the surface of a sample. During deposition, there is an alternating sequence of gaseous chemical precursors that react with the surface of the sample. These

© 2022 The Author(s). Published by Faculty of Engineering, Federal University Oye-Ekiti.
This is an open access article under the CC BY NC license. (https://creativecommons.org/licenses/by-nc/4.0/)

individual gas-surface reactions are called half-reactions (Johnson et al., 2014) and makes up only a part of the material's synthesis. In each half-reaction, the precursor is injected into a chamber (reactor) under vacuum for a designated period to allow the precursor to react fully with the surface via a self-limiting process that leaves only one monolayer at the surface. Subsequently, the chamber is purged with an inert carrier gas (typically $N_2$ or Ar) to remove any residual precursor molecules. Afterward, the counter-reactant precursor pulse and purge are performed, which results in the formation of up to one layer of the desired material. A repeat of the process is then carried out until the required film thickness has been achieved. Therefore, by a careful selection of the number of repetitions of the process, materials with high uniformity and precise thicknesses can be deposited on the surfaces of samples.

### 2.2 $Al_2O_3$ Insulator Deposition Process

An Ultratech Savannah G2 ALD was utilized in this project to grow an $Al_2O_3$ insulating layer onto titanium by subjecting the titanium to alternate pulses of trimethylaluminum (TMA) and $H_2O$ vapour precursors. Firstly, nitrogen gas ($N_2$) was used to purge the ALD chamber of any residual precursor molecules which might have remained from previous depositions. During the TMA exposure (the first half-reaction), the TMA chemisorbed on the titanium surface, leaving the surface coated with a layer of $AlCH_3$ after the reaction had completed. Any remnant of the TMA was purged out of the chamber. The other precursor ($H_2O$ vapour) was then pulsed. The $H_2O$ vapour reacted with the surface – $CH_3$ forming $CH_4$ as a reaction by-product and resulted in a thin $Al_2O_3$ film being formed. The cycle was then further repeated 22 times, with a synthesis of 2 nm thick $Al_2O_3$ being deposited. Fig. 1 (not drawn to scale) illustrates the deposition process and Table 1 shows a summary of the parameters (and their values) used for the process.

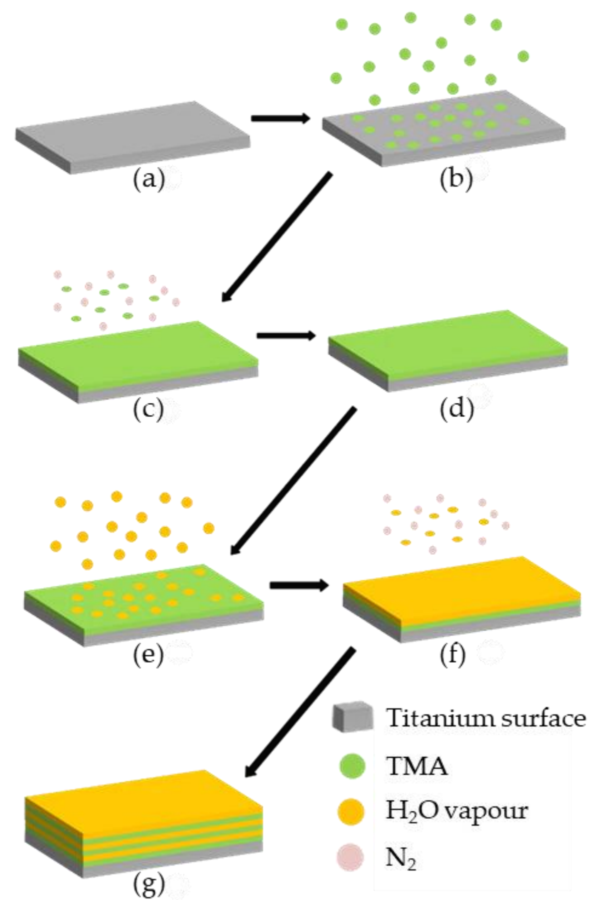


Fig. 1: Schematic diagram of the ALD deposition process for an $Al_2O_3$ film on a titanium surface. Substrate coated with titanium was placed in the ALD chamber (a), and (b) the first precursor (TMA) was pulsed, with the first half-reaction taking place. After the reaction had completed, residues of the TMA were purged out of the chamber using $N_2$ (c). (d) Is the titanium surface covered with ($AlCH_3$) the product of the first half-reaction. The second precursor ($H_2O$ vapour) was pulsed, with the second half-reaction taking place (e). Residues of the $H_2O$ vapour were purged using $N_2$ (f), and (g) a thin $Al_2O_3$ film is formed. The cycle was further repeated 22 times, with a 2 nm thick $Al_2O_3$ layer being achieved.

Table 1. The process parameters used for depositing 2 nm of an $Al_2O_3$ layer

| Parameter | Value |
|---|---|
| $N_2$ flow rate | 20 sccm |
| Stabilise | 5400 sec |
| Pulse 1 (TMA) | 0.015 sec |
| Wait | 5 sec |
| Pulse 2 ($H_2O$ vapour) | 0.015 sec |
| Wait | 5 sec |
| Repeat cycle | 22 cycles |

## 3 Ti/$Al_2O_3$/Pt Diode Fabrication

Fig. 2 (not to scale) shows the process of fabricating the diode (Etor et al., 2016), with the major difference being utilizing $Al_2O_3$ rather than OTS. A two-layer film of approximately 25 nm of titanium metal coated with 100 nm of gold metal was deposited by electron beam evaporation and lift-off (a). In a subsequent photolithographic step, gold was removed by an iodine/potassium-iodide (4:1:8 KI:$I_2$:$H_2O$) wet etch, leaving exposed small areas of titanium (b-c). After removing the photoresist (d) a 2 nm thick of $Al_2O_3$ was then deposited on the exposed titanium (e) using the technique described in Section 2.2 above. After a further photolithographic step, a 40 nm thick layer of platinum was coated on the sample and then patterned through lift-off in the covered regions, resulting in small Ti/$Al_2O_3$/Pt junctions (g-h). Leads and bonding pads were added to conclude the MIM diodes fabrication. A sketch of the device cross-section and an atomic force microscopy (AFM) image of a fabricated structure is shown in Fig. 3. The crossover at the middle of the image is the MIM junction and has a feature size of approximately 10 μm x 10 μm.

## 4 DC Characterization of The Ti/$Al_2O_3$/Pt Diode

The devices were electrically characterized using a parameter analyser. The diodes were tested over a voltage range of ±0.2 V. A typical *J-V* characteristic of the diode is plotted in Fig. 4, showing a strong non-linearity at zero-bias (i.e., $V = 0$ V). The zero-bias curvature coefficient

© 2022 The Author(s). Published by Faculty of Engineering, Federal University Oye-Ekiti.
This is an open access article under the CC BY NC license. (https://creativecommons.org/licenses/by-nc/4.0/)

http://doi.org/10.46792/fuoyejet.v7i2.815 http://journal.engineering.fuoye.edu.ng/

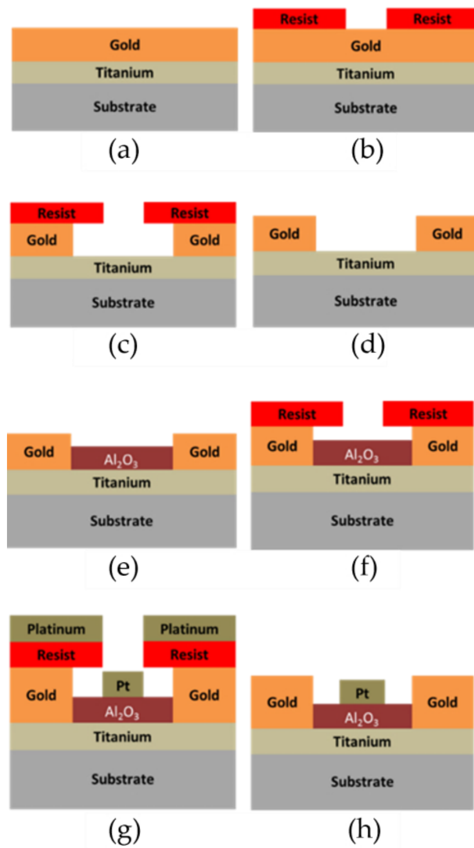


Fig. 2: Fabrication process for the Ti/$Al_2O_3$/Pt MIM diode. (a) Ti/Au two-layer on borosilicate glass. Photolithographic patterning (b) followed by gold wet etching (c). Photoresist removal (d) and $Al_2O_3$ deposition (e). Photolithographic patterning (f), Pt coating (g) and lift-off (h).

($\gamma_{ZB}$), a figure of merit for MIM junctions, as can be seen in Fig. 5, is approximately 5.4 $V^{-1}$.

Curvature coefficient, $\gamma$, is a measure of the non-linearity of the rectifier *I-V* characteristic at a given point, expressed in Eq. 1 (Etor et al., 2016)) and affects rectified current in MIM diodes. The $\gamma$ can be obtained at any desired voltage but is more useful at zero-bias especially for applications like energy detection or harvesting where there would not be biasing when in operation (Etor et al., 2016).

$$\gamma = N_L R_v|_{V=V_g} \quad (1)$$

where $N_L$ is the non-linearity of the rectifier at a particular voltage $V_g$, as expressed in Eq. 2 (Etor et al., 2016).

$$N_L = \left.\frac{d^2 I}{dV^2}\right|_{V=V_g} \quad (2)$$

and $R$ the rectifier resistance at a particular voltage $V_g$, defined by Eq. 3 (Etor et al. (2016)).

$$R = \left.\left(\frac{dI}{dV}\right)^{-1}\right|_{V=V_g} \quad (3)$$

The parameters stated above can be extracted directly via electrical measurement or from polynomial fitting to the rectifier *I-V* characteristic raw results (Etor et al. (2016)). The typical Ti/$Al_2O_3$/Pt device resistance as a function of voltage is shown in Fig. 6, with the zero-bias resistance ($R_{ZB}$) being approximately 118 kΩ, a value considerably smaller than other MIM diode topologies and that allows more current to be rectified.

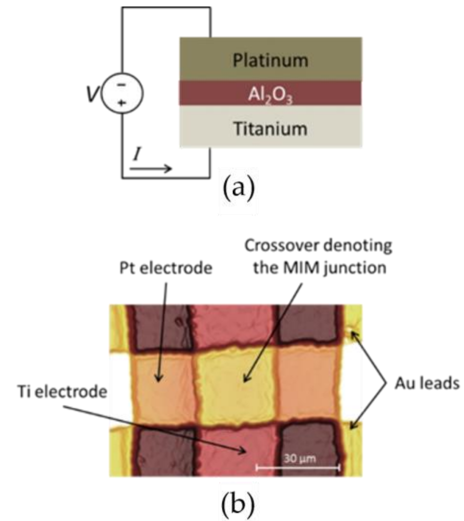


Fig. 3: A sketch of the device cross-section (a) and an AFM image of a fabricated Ti/$Al_2O_3$/Pt structure (b). The titanium and platinum electrodes act as the anode and the cathode, respectively.

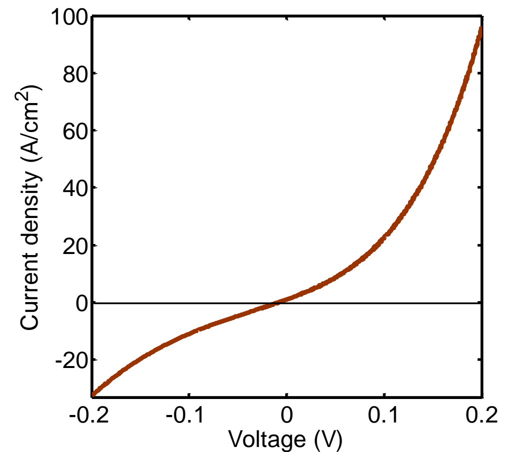


Fig. 4: Typical *J-V* characteristics of a manufactured Ti/$Al_2O_3$/Pt MIM diode.

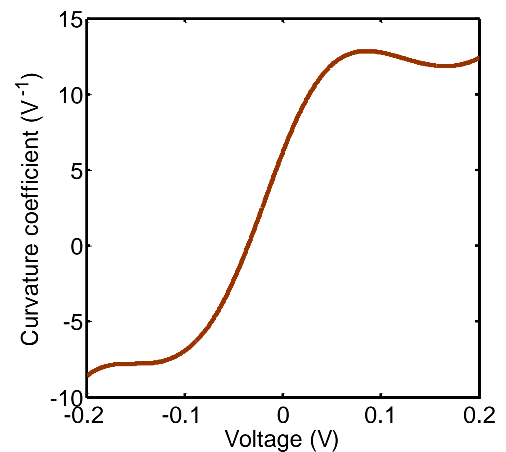


Fig. 5: Typical curvature coefficient plot of a manufactured Ti/$Al_2O_3$/Pt MIM diode.

© 2022 The Author(s). Published by Faculty of Engineering, Federal University Oye-Ekiti.
This is an open access article under the CC BY NC license. (https://creativecommons.org/licenses/by-nc/4.0/)

http://doi.org/10.46792/fuoyejet.v7i2.815 http://journal.engineering.fuoye.edu.ng/

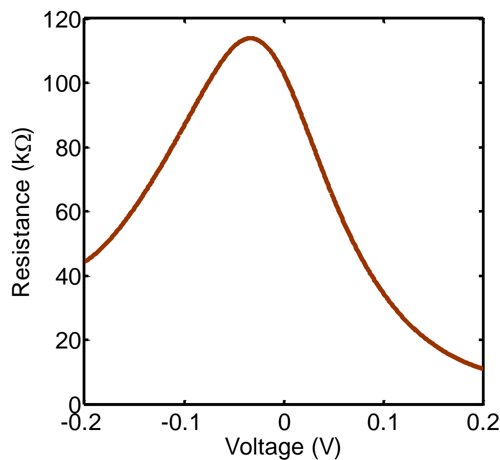


Fig. 6: Typical resistance plot of a manufactured Ti/$Al_2O_3$/Pt MIM diode.

## 5 Comparison Between the DC Electrical Parameters of $Al_2O_3$ Insulator Diode and OTS Insulator Diode

To measure how the performance of the fabricated Ti/$Al_2O_3$/Pt MIM diode competes with other MIM diode topologies, the DC electrical parameters of the (Ti/$Al_2O_3$/Pt) diodes were compared with the DC electrical parameters of our OTS MIM diode (Ti/OTS/Pt) topology fabricated and reported previously in (Etor et al. (2016)). Shown in Fig. 7 are the typical *J-V* curves of the OTS and $Al_2O_3$ diodes. As can be seen, the two *J-V* characteristics look similar; however, the $Al_2O_3$ insulator diode has a slightly higher current density than the OTS insulator diode. The $Al_2O_3$ diodes were also found to have more uniform electrical results than the OTS diodes. This can be seen in Table 2. The table shows the average values of zero-bias curvature coefficient ($\gamma_{ZB}$), current ratio, current density, and throughput (with the standard deviation in those results shown in brackets). The more uniform results and improved current density associated with the $Al_2O_3$ diodes are due to the high precision of the $Al_2O_3$ film deposition performed using the ALD.

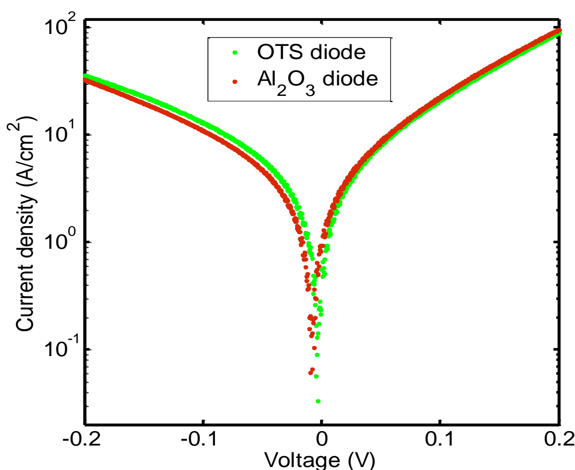


Fig. 7: Typical J-V curves of the OTS and $Al_2O_3$ insulator diodes.

Table 2. Comparison of electrical parameters between OTS and $Al_2O_3$ diodes (128 OTS and 128 $Al_2O_3$ diodes were used for this comparison)

| Parameter | 2 nm OTS insulator diode | 2 nm $Al_2O_3$ insulator (ALD) diode |
|---|---|---|
| Average $\gamma_{ZB}$ ($V^{-1}$) | 5.6 | 5.9 |
| Average $\gamma_{ZB}$ ($V^{-1}$) | 3.5 (0.4) | 3.8 (0.2) |
| Average current ratio | 1.8 (0.5) | 1.8 (0.3) |
| Average current density (A/cm²) | 49 | 56 |
| Throughput (%) | 78 | 82 |

## 4 Conclusion

The production and DC electrical characterization of MIM diodes with $Al_2O_3$ insulator, deposited using the ALD, has been presented. The DC analysis showed that the devices have strong non-linear *J-V* characteristics with typical zero-bias curvature coefficient ($\gamma_{ZB}$) and resistance of approximately 5.4 $V^{-1}$ and 118 kΩ respectively. A comparison between the DC electrical results of the manufactured $Al_2O_3$ insulator diodes and OTS insulator diodes were made, with the $Al_2O_3$ insulator diodes producing slightly better results, including current density, zero-bias curvature coefficient and yield. Although the DC electrical results of the $Al_2O_3$ insulator diodes here are slightly better, the advantages the OTS insulator diodes present, such as low-cost of production, low-temperature manufacturing process and the possibility it presents for the roll-to-roll volume manufacture of MIM devices, cannot be ignored. It will be a case of making a choice between a slight improvement in electrical parameters and a huge difference in production cost, with the OTS device being the cheaper one.

## References


Chalker, P. R., Romani, S., Marshall, P. A., Rosseinsky, M. J., Rushworth, S. & Williams, P. A. (2010). Liquid Injection Atomic Layer Deposition of Silver Nanoparticles. *Nanotechnology*, 21, 405602. https://iopscience.iop.org/article/10.1088/0957-4484/21/40/405602

Denisov, V. I., Zakhar'yash, V. F., Klement'ev, V. M. & Chepurov, S. V. (2007). Very-high-speed metal-oxide-metal diodes on W-Ni, Pt-Ti, and Pt-W contacts. *Instruments & Experimental Techniques*, 50, 517-523. https://doi.org/10.1134/S002044120704015X

Dodd, L. E., Gallant, A. J. & Wood, D. (2012). Ti-TiOx-Pt Metal-Oxide-Metal Diodes Fabricated Via a Simple Oxidation Technique. *MRS Proceedings*, 1415, 91-96. http://dx.doi.org/10.1557/opl.2012.72

Drullinger, R. E., Evenson, K. M., Jennings, D. A., Petersen, F. R., Bergquist, J. C., Burkins, L. & Daniel, H.U. (1983). 2.5 THz Frequency Difference Measurements in the Visible Using Metal-Insulator-Metal Diodes. *Applied Physics Letters*, 42, 137-138. https://doi.org/10.1063/1.93852

Etor, D., Dodd, L. E., Balocco, C. & Wood, D. (2019). Conduction mechanisms in metal/self-assembled monolayer/metal junctions. *IET Micro & Nano Letters*, 14, 808 – 811. https://doi.org/10.1049/mnl.2018.5747

Etor, D., Dodd, L. E., Wood, D. & Balocco, C. (2016). An Ultrathin Organic Insulator for Metal–Insulator–Metal Diodes. *IEEE*


© 2022 The Author(s). Published by Faculty of Engineering, Federal University Oye-Ekiti.
This is an open access article under the CC BY NC license. (https://creativecommons.org/licenses/by-nc/4.0/)

*Transactions on Electron Devices*, 63(7), 2887-2891. https://doi.org/10.1109/TED.2016.2568279

Etor, D., Dodd, L. E., Wood, D. & Balocco, C. (2016). High-Performance Rectifiers Fabricated on a Flexible Substrate. *Applied Physics Letters*, 109, 193110. https://doi.org/10.1063/1.4967190

Evenson, K. M., Jennings, D. A. & Petersen, F. R. (1984). Tunable far-infrared spectroscopy. *Applied Physics Letters*, 44, 576. https://doi.org/10.1063/1.94845

Evenson, K. M., Wells, J. S., Matarrese, L. M. & Elwell, L. B. (1970). Absolute Frequency Measurements of the 28- And 78-mm cw Water Vapor Laser Lines. *Applied Physics Letters*, 16, 159. https://doi.org/10.1063/1.1653143

Gordon, P. G., Kurek, A. & Barry, S. T. (2015). Trends in Copper Precursor Development for CVD and ALD Applications. *ECS J. Solid State Science & Technology*, 4, 3188-3197. http://dx.doi.org/10.1149/2.0261501jss

Griffiths, M. B. E., Pallister, P. J., Mandia, D. J. & Barry, S. T. (2016). Atomic Layer Deposition of Gold Metal. *Chemistry of Materials*, 28, 44–46. https://doi.org/10.1021/acs.chemmater.5b04562

Hausmann, D. M., Kim, E., Becker, J. & Gordon, R. G. (2002). Atomic Layer Deposition of Hafnium and Zirconium Oxides Using Metal Amide Precursors. *Chemistry of Materials*, 14, 4350-4358. https://doi.org/10.1021/cm020357x

Hemmetter, A., Yang, X., Wang, Z., Otto, M., Uzlu, B., Andree, M., Pfeiffer, U., Vorobiev, A., Stake, J., Lemme, M. C., & Neumaier, D. (2021). Terahertz Rectennas on Flexible Substrates Based on One-Dimensional Metal–Insulator–Graphene Diodes. *ACS Applied Electronic Materials*, 3, 9, 3747–3753. https://doi.org/10.1021/acsaelm.1c00134

Jinpeng, S., Xin'an, Y., Shan, L., Hongqiang, Z., Jinfeng, H., Xin, Y., Xiaoxing, F. & Binjie, G. (2012). Design and implementation of an ultra-low power passive UHF RFID tag. *Journal of Semiconductor*, 33, 115011-1–115011-5. https://ur.booksc.me/book/37805625/55c8f8

Johnson, R. W., Hultqvist, A. & Bent, S. F. (2014). A Brief Review of Atomic Layer Deposition: From Fundamentals to Applications. *Materials Today*, 17, 236-246. https://doi.org/10.1016/j.mattod.2014.04.026

Kariniemi, M., Niinisto, J., Hatanpaa, T., Kemell, M., Sajavaara, T., Ritala, M. & Leskela, M. (2011). Plasma-Enhanced Atomic Layer Deposition of Silver Thin Films. *Chemistry of Materials*, 23, 2901–2907. https://doi.org/10.1021/cm200402j

Kukli, K., Ritala, M., Schuisky, M., Leskelä, M., Sajavaara, T., Keinonen, J., Uustare, T. & Hårsta, A. (2000). Atomic Layer Deposition of Titanium Oxide from $TiI_4$ and $H_2O_2$. *Chemistry of Vapor Deposition*, 6(6), 303-310. https://doi.org/10.1002/1521-3862(200011)6:6%3C303::AID-CVDE303%3E3.0.CO;2-J

Mitrovic, I. Z., Almalki, S., Tekin, S. B., Sedghi, N., Chalker, P. R., & Hall, S. (2021). Oxides for Rectenna Technology. *Materials*, 14(18), 5218. https://doi.org/10.3390/ma14185218

Niskanen, A., Hatanpää, T., Arstila, K., Leskela, M. & Ritala, M. (2007). Radical-Enhanced Atomic Layer Deposition of Silver Thin Films Using Phosphine-Adducted Silver Carboxylates. *Chemistry of Vapor Deposition*, 13, 408–413. https://doi.org/10.1002/cvde.200606519

Pan, Y., Powell, C. V., Song, A. M. & Balocco, C. (2014). Micro Rectennas: Brownian Ratchets for Thermal-Energy Harvesting, *Applied Physics Letters*, 105, 253901. https://doi.org/10.1063/1.4905089

Periasamy, P. Berry, J. J., Dameron, A. A., Bergeson, J. D., Ginly, D. S., O'Hayre, R. Y., & Parilla, P. A. (2011). Fabrication and Characterization of MIM Diodes Based on $Nb/Nb_2O_5$ Via a Rapid Screening Technique. *Advances in Materials*, 23, 3080–3085. https://onlinelibrary.wiley.com/doi/abs/10.1002/adma.201101115

Sakuma, E. & Evenson, K. M. (1974). Characteristics of tungsten-nickel point contact diodes used as laser harmonic-generator mixers. *IEEE Journal of Quantum Electronics*, 10, 599–603. https://doi.org/10.1109/JQE.1974.1068209

Wang, X., Tabakman, S. M. & Dai, H. (2008). Atomic Layer Deposition of Metal Oxides on Pristine and Functionalized Graphene. *Journal of American Chemical Society*, 130, 8152–8153. https://doi.org/10.1021/ja8023059

© 2022 The Author(s). Published by Faculty of Engineering, Federal University Oye-Ekiti.

This is an open access article under the CC BY NC license. (https://creativecommons.org/licenses/by-nc/4.0/)